Combinatorial computational chemistry approach to the design of metal catalysts for deNO$_x$

Akira Endou[a], Changho Jung[a], Tomonori Kusagaya[a], Momoji Kubo[a],
Parasuraman Selvam[b], Akira Miyamoto[a,b,*]

[a]Department of Materials Chemistry, Graduate School of Engineering, Tohoku University, Aoba-yama 07, Sendai 980-8579, Japan
[b]New Industry Creation Hatchery Center, Tohoku University, Aoba-yama 04, Sendai 980-8579, Japan

Abstract

Combinatorial chemistry is an efficient technique for the synthesis and screening of a large number of compounds. Recently, we introduced the combinatorial approach to computational chemistry for catalyst design and proposed a new method called "combinatorial computational chemistry". In the present study, we have applied this combinatorial computational chemistry approach to the design of precious metal catalysts for deNO$_x$. As the first step of the screening of the metal catalysts, we studied Rh, Pd, Ag, Ir, Pt, and Au clusters regarding the adsorption properties towards NO molecule. It was demonstrated that the energetically most stable adsorption state of NO on Ir model cluster, which was irrespective of both the shape and number of atoms including the model clusters.
© 2003 Elsevier B.V. All rights reserved.

Keywords: Combinatorial computational chemistry; Density functional calculation; Adsorption; Precious metal particles

1. Introduction

Combinatorial chemistry now plays an important role in the lead discovery and hit optimization processes not only in the pharmaceutical chemistry but also other areas such as catalysis, materials chemistry and so on [1–3]. Combinatorial chemistry is a methodology where a large number of new catalytic materials are prepared and tested in a parallel way. Although significant progress has been made on the fundamental understanding of catalysis, the development of new catalysts still depends very much on previous accumulated experience, intuition, a large amount of experimental work and some serendipity. On the other hand, if a systematic study of the potential variable that can influence the catalyst behavior has to be carried out, a very large number of experiments with large times of research and development are required. The global search and optimization strategy used for the experimental design is the main difference with the traditional research and allows to reduce the number of experiments needed to find an optimal catalyst composition. Combinatorial catalysis involves the coordination of high-throughput systems for preparation, characterization, catalyst testing, large information data management, and rapid screening and optimization techniques. In the last few years, combinatorial methods have extensively been used to identify, optimize, and rationally select heterogeneous catalysts. Notwithstanding the impressive

advances in this field, the efficiency of available methods for preparing and testing heterogeneous catalysts is rather low relative to homogeneous catalysts. On the other hand, with the advent of the remarkable advancements in the computational chemistry with respect to the development of both the theory and calculation methods show promise. Furthermore, computational chemistry has effectively been used to elucidate, for instance, the catalytic activity, the catalyst deactivation, and the mechanism of catalytic reactions, etc. Such studies at atomic and electronic levels are expected to play an important role to predict new catalysts with high activity, selectivity and resistance to poisoning. It is in this context, we introduced recently the concept of combinatorial approach to computational chemistry for the catalyst design and proposed a new method called ''combinatorial computational chemistry'' [4,5]. Accordingly, a large number of metals, supports, and additives on the catalytic activity can systematically be investigated using computer simulation techniques.

Over the past few decades, considerable efforts have been focused on the development of automotive exhaust catalysts. The introduction of stringent emission standards for the vehicular emissions, viz. carbon monoxide (CO), hydrocarbons (HC) and nitrogen oxides (NO_x), has led to extensive research activities on the development of automotive pollution control three-way catalyst (TWC) systems [6–13]. The traditional TWC are not available in steady-state lean-burning engines [14]. On the other hand, studies on zeolite-based catalysts, e.g. metal ion-exchanged ZSM-5, have shown to be exceptionally active for the $deNO_x$ reaction [15,16]. However, the use of our new combinatorial computational chemistry concept for the search of viable $deNO_x$ catalysts resulted in trivalent cation-exchanged ZSM-5 catalysts, viz. Cr-ZSM-5, Fe-ZSM-5, Ir-ZSM-5 and Tl-ZSM-5, as potential candidates for $deNO_x$ reactions with high resistance to water and sulfur oxides [4]. These results, in particular for the Fe- and Ir-containing ZSM-5, are well supported by experiments [17–20]. It is also noteworthy here that the other two systems have not been investigated experimentally. It is, however, to be noted here that the zeolite-based catalysts possess low stability under realistic situations, i.e. thermal and hydrothermal conditions. Therefore, from the view point of the lifetime of the catalysts, the use of

noble-metal supported metal oxide catalyst systems are more effective and gaining considerable interest as selective catalytic reduction (SCR) of NO_x emission. They are also promising for the lean-burning of NO_x due to their low light-off temperature and relatively high hydrothermal stability.

Recently, a new type of precious metal-based catalyst supported on metal oxide was industrialized in Japan for lean-burn engines [22,23]. Most of these studies were performed employing Pt, Pd and Rh. However, in recent years, the interest in Ir-based catalysts has been increasing steadily as they exhibit high activity for the NO reduction and especially unsupported Ir was shown to exhibit excellent activity [19–22]. In this context, it is noteworthy here that we have also reported a similar observation on the adsorption characteristics of NO over noble-metal clusters by density functional calculations [24,25]. In continuation of our interest in combinatorial computational chemistry to design new catalyst systems for a variety of problems [4,5], we extend this study to noble-metal catalysts for the $deNO_x$ reaction. As a first step of screening of the metal catalysts for the SCR process of NO_x, we target the catalytic activity of noble-metal catalysts for the reduction of NO with a special emphasis on the adsorption characteristics. Further, the influence of the metal cluster shape and size on the adsorption properties towards NO will be investigated.

2. Method

All Kohn–Sham calculations were performed using the ADF program [26] developed at Vrije University, Amsterdam. The double-ζ (DZ) basis sets were applied to all precious metals, while for the nitrogen and oxygen atoms, the triple-ζ plus double polarization functions (TZpp) basis sets were used. For the calculations, which include the precious metal atoms, scalar relativistic corrections within Pauli formalism were also considered. The local density approximation (LDA) with the Vosko–Wilk–Nusair local functional [27] was used to optimize the geometries. Energies for optimized geometries were evaluated using the generalized gradient approximation (GGA) with the Becke's exchange functional and the Perdew correlation functional [28] (denoted as BP). In a previous

study [25], we have already validated the above computational conditions because the geometry and the binding energy of the Ir cluster and the NO/Ir system obtained using the LDA (the binding energy was reevaluated using the GGA) agreed well with those obtained using the full GGA. Atomic charges and molecular charges were estimated using the Mulliken population analysis.

3. Models

For the adsorbate molecule, a full geometry optimization with $C_{\infty v}$ symmetry was carried out to determine the structure of the NO molecule in the gas phase. The equilibrium internuclear distance of N–O bond was equal to 1.149 Å, which is close to the experimental value of 1.151 Å [29]. It was also found that the N–O bond distance obtained here agrees well with previously reported results [30,31]. The calculated value of the v_{NO} was 1943 cm^{-1}, which is in accordance with the experimental frequency 34 of 1904 cm^{-1}. Six noble-metal clusters were selected in the present study: Rh, Pd, Ag, Ir, Pt, and Au. In order to represent real catalytic metal systems, clusters containing dozens of metal atoms should be considered. However, one may be able to adopt a much smaller cluster as a representative of such catalytic species when the interactions between the supported metal particle and the adsorbed reactant molecule in the local field of the catalyst surface is mainly focused on. Furthermore, it is likely that they can also represent as a model of ultrafine clusters. Such a choice could be further justified by the relatively small tetrahedral clusters of Ir supported on MgO [32,33] and on γ-Al$_2$O$_3$ and on [34,35], which have been characterized by extended X-ray absorption fine structure (EXAFS) spectroscopy. Based on these findings, we previously reported that the adsorption characteristics of the precious metal tetrahedral tetraatomic clusters [24] (denoted as M$_4$, M = Rh, Pd, Ag, Ir, Pt, and Au) towards NO, with combinatorial computational approach by using the density functional calculations. In this previous study, we already validated our computational conditions and the tetrahedral tetraatomic clusters.

In this investigation, we considered pentaatomic metal clusters (denoted by M$_5$; M = Rh, Pd, Ag, Ir,

Table 1
Interatomic distances ($R_{M–M}$), binding energies (BE), and spin properties for the ground states of various M$_5$ clusters

M	$R_{M–M}$ (Å)	BE (kcal/mol)	Spin multiplicity
M$_5$(sp) clusters			
Rh	2.402	468.3	Sextet
Pd	2.618	222.9	Triplet
Ag	2.638	144.7	Doublet
Ir	2.552	456.8	Quartet
Pt	2.617	329.7	Triplet
Au	2.807	173.2	Doublet
M$_5$(tb) clusters			
Rh	2.402	462.2	Octet
Pd	2.618	225.5	Triplet
Ag	2.638	145.3	Doublet
Ir	2.552	447.9	Quartet
Pt	2.617	327.2	Triplet
Au	2.807	177.8	Doublet

Pt, and Au) where more freedom regarding the cluster geometry and the mode of adsorption could be anticipated. Accordingly, there exist two possible structures for M$_5$ clusters, viz. square pyramidal and trigonal bipyramidal denoted as M$_5$(sp) and M$_5$(tb), respectively. The detail of these pentaatomic clusters in the cases of M = Ir, Pt, and Au were already reported by our group [25]. The optimized geometries, binding energies, and spin multiplicities for M$_5$(sp) and M$_5$(tb) clusters are summarized in Table 1. From the previous study reported by another group [36], clusters with n = 4–6 were shown to be planar. In that study, the square pyramidal Pt$_5$ cluster was less stable than the trigonal bipyramidal Pt$_5$ cluster by ca. 1.38 kcal/mol. The energy difference between those clusters is close to our present result (2.51 kcal/mol) although the order of stability in the present study is opposite to that previously reported [36]. It is not straightforward to compare present results (Table 1) with the others [36] because of the different calculation conditions such as exchange–correlation functionals. On the other hand, to the best of our knowledge, there are no published calculations for Rh$_5$, Pd$_5$, Ag$_5$, Ir$_5$, and Au$_5$ clusters. In order to discuss the energetics of the NO/metal cluster systems, several initial geometries of NO toward M$_5$(sp) and M$_5$(tb) clusters were taken into account. At first, three possible initial structures were considered for M$_5$-type cluster models (Fig. 1): (a) NO molecule
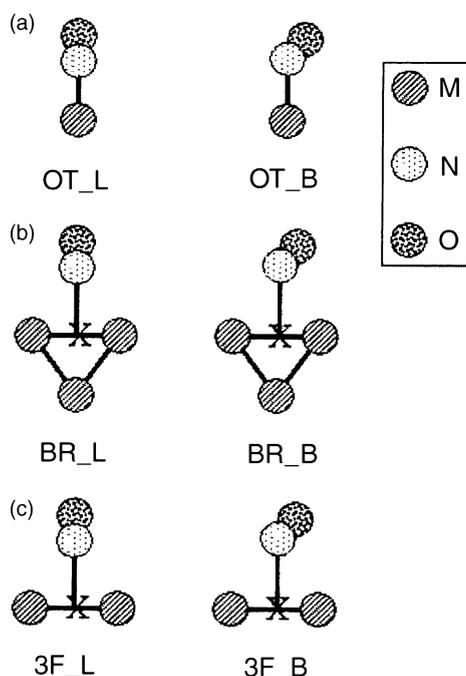
Fig. 1. Schematic representation of initial geometries of NO molecule on M_5(sp) clusters: (a) NO on top M with linear geometry (OT_L) and on top M with bent geometry (OT_B); (b) NO on top of bridge site of M with linear (BR_L) and with bent geometry (BR_B); and (c) NO on top of the three-fold site of M with linear geometry (3F_L) and with bent geometry (3F_B). See also the text.

located on top of the apical atom (denoted as OT_L); (b) NO molecule located on top of the bridge site in which the NO molecule is located in the same plane as three metal atoms (denoted as BR_L); and (c) on the three-fold site (denoted as 3F_L). In all the cases, the initial angle of O–N–M was $180.0°$. The corresponding model of NO with bend geometry is reported as OT_B, BR_B and 3F_B, respectively, with an initial O–N–M angle equal to $165.0°$. Full geometry optimizations starting from the OT_L BR_L and 3F_L structures for the NO/M_5(sp) systems were done by adopting C_{4v}, C_s, and C_s symmetries, respectively. As for the NO/M_5(tb) systems, full geometry optimizations were done, starting from OT_L, BR_L and 3F_L structures with the adoptation of C_{3v}, C_s, and C_s symmetries, respectively. Experimentally, the NO molecule tends to adsorb on various metals with respect to the surface normal vector, although some exceptions have also been reported, e.g. NO/Pt(1 1 1) [37].

For the full geometry optimizations of these initial structures of OT_B, BR_B and 3F_B, C_s, C_s and C_s symmetries were applied, respectively.

4. Results and discussion

4.1. Adsorption states of NO on M_5(sp) clusters

The adsorption energies (E) of NO molecules on square pyramidal clusters, M_5(sp) obtained by starting from six initial geometries (see Fig. 1) are listed in Table 2. The E_{ads} values in the present study are deduced

$$E_{ads} = E_{M–NO} − (E_M + E_{NO}) \tag{1}$$

where $E_{M–NO}$, E_M, and E_{NO} correspond to the binding energies of NO adsorbed on M, M_5(sp) cluster, and free NO molecule, respectively. The negative E_{ads} values indicate that the adsorbed state (M–NO) is energetically favorable.

In our previous study [24], the stability of the NO adsorption state on tetrahedral Rh_4 and Pd_4 clusters was compared with that obtained by DFT calculations under the periodic boundary conditions [38], in order to verify the suitability of the relatively simple models to investigate NO/precious metal systems. In this study, again, let us discuss the E_{ads} values for the NO/M_5(sp) systems in the cases of M = Rh and Pd. The maxima of the absolute E_{ads} values in the series of

Table 2
Adsorption energies (E_{ads}; kcal/mol) of NO on various M_5 clusters

M	OT_L	OT_B	BR_L	BR_B	3F_L	3F_B
M_5(sp) clusters						
Rh	−62.9	−54.0	−55.5	−55.4	−43.1	−53.8
Pd	−47.5	−42.3	−47.5	−47.7	−29.8	−33.1
Ag	−25.8	−22.7	−25.0	−24.1	−22.8	−25.1
Ir	−78.9	−79.6	−43.9	−43.5	−41.5	−38.7
Pt	−58.7	−57.5	−45.0	−42.9	−24.5	−57.0
Au	−29.5	−29.6	−31.5	−31.5	−28.4	−28.4
M_5(tb) clusters						
Rh	−62.2	−55.7	−62.0	−61.1	−50.0	−59.6
Pd	−52.6	−51.9	−45.0	−45.2	−34.4	−38.7
Ag	−9.93	−5.59	−21.2	−22.6	−30.9	−31.2
Ir	−73.7	−71.6	−53.9	−54.0	−31.7	−51.6
Pt	−61.5	−58.4	−47.5	−47.3	−26.1	−26.5
Au	−6.69	−27.5	−30.2	−15.7	−22.4	−22.7

various initial geometries for the NO/Rh_5(sp) and NO/Pd_5(sp) systems are -62.9 and -47.7 kcal/mol, respectively. This tendency can be compared with that reported by Loffreda et al. [38]. They reported that the energetic stability of the NO adsorption states on the Rh surfaces was higher than that on the Pd surfaces. Thus, our present results based on simple models is suitable in order to further discuss the energetics for the NO/precious metal clusters systems.

The E_{ads} values shown in Table 2 for the NO/Rh_5(sp) systems evidently indicate that the linear adsorption mode of the NO molecule on top of the apical Rh atom (OT_L) cluster is the most energetically favorable (-62.9 kcal/mol). The interatomic distance of the Rh–N bond is 1.760 Å and agrees well with that reported by Tsai and Hass (1.747 Å) [39]. The atomic charge on the apical Rh atom is $+0.06$ in spite of the formation of the relatively strong Rh–N bond as expected by the E_{ads} value. This probably indicates the balance between the donation and the back-donation of electrons in this system. Regarding the NO/Pd_5 system, it is clear that the bridged adsorption state of the NO molecule (BR_B) is energetically stable (-47.7 kcal/mol). The interatomic distances of two Pd–N bonds are 1.895 and 1.891 Å, which qualitatively agree with those calculated by Mannstadt and Freeman (1.850 Å) [40]. The atomic charges on these two Pd atoms are $+0.19$ and $+0.19$, respectively. Interestingly, the substantial change in the shape of the Pd_5 cluster was observed upon the NO adsorption. The final shape in this state resembles with that of the Pd_5(tb) cluster. In the series of the NO/Ag_5(sp) systems, similar to the case of the NO/Rh_5(sp) systems, the linear adsorption mode of the NO molecule on top of the apical Ag atom is the most favorable (-25.8 kcal/mol). The interatomic distance of the Ag–N bond is 1.919 Å. The charge on the apical Ag atom is -0.23 and involves that the degree of the donation of electrons from the adsorbed NO molecule to the Ag cluster is large. Comparing the absolute values of E_{ads} for the NO/M_5(sp) systems with the M = Rh, Pd, and Ag, the order of energetic stability of NO/M_5(sp) systems follows as is Rh > Pd > Ag, which agrees well with that obtained for NO/tetrahedral M_4 clusters systems [24].

Next, the E_{ads} values in the series of Ir, Pt, and Au are compared. It can be seen from Table 2 that for the NO/Ir_5 indicate that the adsorption mode of NO

derived from the OT_B initial geometry is energetically favorable. The Ir–N distance is 1.760 Å and the atomic charge on the apical Ir atom, which is directly bound to the N atom is $+0.18$. In the case of the NO/Pt_5(sp) system, the linear adsorption state of the NO molecule on the apical Pt atom is ergetically stable. The bond distance of the Pt–N bond is 1.774 Å. This value is the completely same as that estimated for the NO/M_4 clusters systems [24] and is approximately 0.03 and 0.06 Å shorter than those reported in [39,40], respectively. The atomic charge on the apical Pt atom in this system is $+0.17$. In the case of the NO/Au_5(sp) systems, the bent adsorption mode of the NO molecule (BR_L) is the most stable (-31.5 kcal/mol). The interatomic distance of the Au–N bond is 1.982 Å, which is relatively longer than that of the Ir–N or Pt–N bond. Interestingly, the coordination number of the NO molecule to the Au_5 cluster is always 1, within the range of this study. The possibility of the formation of more than two Au–N bonds using constrained geometry optimization was not studied. Comparing the absolute values of E_{ads} for the NO/M_5(sp) systems, the stability is given as Ir > Pt > Au.

Based on the entire comparison of the E_{ads} values listed in Table 2, it is clear that the order of the energetic stability of the adsorption states of the NO molecules on the M_5(sp) clusters can be described as Ir > Rh > Pt > Pd > Au > Ag, which is in accordance with that of NO/tetrahedral M_4 clusters systems excepts that the order of Au and Ag is interchanged.

In terms of the electronic populations estimated by the Mulliken population analysis, one plausible explanation regarding the energetic stability of the NO/M_5 systems was attempted (Table 3). To simplify the analyses, most thermodynamically favorable adsorption states of the NO molecules on each M_5(sp) cluster obtained using various initial geometries were used. From the inspection of Table 3, it is found that the NO/M_5(sp) systems with M = Rh, Ir, and Pt show donation and π back-donation (approximately 0.2–0.3 electrons from the 5σ orbital to the metal atom and 0.2–0.6 electrons from the metal atom to the $2\pi^*$ orbital of the NO molecule, respectively), which is in agreement with the Blyholder model [41]. The direct comparison of the present results shown in Table 3 with those reported using slab models with the DFT calculations under PBC may not be straight

Table 3
Electronic population of selected orbitals for NO molecule in the gas phase and NO/M_5 systems

Adsorption state	M	5σ	$2\pi^*$
M_5(sp) clusters			
OT_L	Rh	1.82	1.18
BR_B	Pd	1.74	0.89
OT_L	Ag	1.86	0.90
OT_B	Ir	1.86	1.18
OT_L	Pt	1.84	1.68
BR_L/BR_B	Au	1.77	0.95
M_5(tb) clusters			
OT_L	Rh	1.86	1.44
OT_L	Pd	1.70	2.44
3F_B	Ag	1.56	1.00
OT_L	Ir	1.70	1.92
OT_L	Pt	1.68	1.78
BR_L	Au	1.77	1.02
NO in gas phase		2.00	1.00

Each stable adsorption state of NO/M_5 systems in Table 2 was chosen.

forward. At least, nevertheless, part of the present results may be able to compare with those estimated by Loffreda et al. [38]. They reported that the electronic populations of the NO molecules regarding the 5σ and $2\pi^*$ orbitals, which adsorbed on top of the Rh(1 0 0) surfaces with 0.5 ML of NO coverage, were 1.78 and 1.22, respectively. In the present study, the NO/Rh_5(sp) system shows the similar behavior regarding the donation and r back-donation, as shown in Table 3. This justifies to adopt such analyses for the present small cluster systems. Surprisingly, however, the donation of electrons from the $2\pi^*$ orbital of the adsorbed NO molecules to the metal atom was also observed. The charges donated from the $2\pi^*$ orbitals to the precious metal atom in the NO/Au_5(sp), NO/Ag_5(sp), and NO/Pd_5(sp) systems were 0.05, 0.10, and 0.11, respectively. In the cases of the NO/Ag_5(sp) and NO/Au_5(sp) systems, such interesting behavior regarding the donation of the $2\pi^*$ electrons may be the one possible reason why the Ag and Au atoms, which were bound to the N atom, possess negative atomic charges (−0.23 and −0.02, respectively).

4.2. Adsorption states of NO on M_5(tb) clusters

Table 2 summarizes the adsorption states of NO molecules on the trigonal bipyramid al clusters

M_5(tb). The initial geometries were chosen in the same manner as the previous ones.

From the E_{ads} values shown in Table 2 for the NO/Rh_5(tb) systems, it is clearly seen that the linear adsorption mode of the NO molecule on top of the apical Rh atom of the Rh_5(tb) cluster is the most energetically stable (−62.2 kcal/mol). This value is very close to that observed in the NO/Rh_5(sp) systems (−62.9 kcal/mol). The distance of the Rh–N bond is 1.735 Å, which is slightly shorter than that of the NO/Rh_5(sp) system (1.760 Å). The atomic charge on the apex of this Rh_5(tb) cluster is +0.14. In the case of the NO/Pd_5(tb) systems, the E_{ads} values show that the linear adsorption state of the NO molecule, which is the same as that in the case of the NO/Rh_5(tb) systems, is the most energetically favorable (−52.6 kcal/mol). The interatomic distance of the Pd–N bond is 1.742 Å and is in accordance with that reported in [39] (1.760 Å). This bond distance is approximately 0.15 Å longer than that of the NO/Pd_5(sp) systems, which corresponds to the higher stability of the NO/Pd_5(tb) system due to the formation of the stronger Pd–N bond. The atomic charge on the apical Pd atom in the linear adsorption mode of the NO molecule on the Pd_5(tb) cluster is +0.18. Regarding the case of the NO/Ag_5(tb) systems, it is found that the slightly bent adsorption mode on the three-fold site of the Ag_5(tb) cluster is the most stable (−31.2 kcal/mol). The interatomic distances between three Ag atoms and the N atom are 2.463, 2.463, and 2.344 Å. These suggest the relatively weak interaction of the NO molecule with the Ag_5(tb) clusters. This may also be supported by the substantially small values of the atomic charge on these three Ag atoms (+0.06).

Comparing the absolute E_{ads} values for the NO/M_5(tb) systems with M = Rh, Pd, and Ag, it can be understood that the order of the thermodynamic stability on the NO/M_5(tb) systems studied is Rh > Pd > Ag, which is the same with that described for the NO/M_5(sp) systems. The order of the interatomic distances of the N-precious metal atom bonds, similar to the case of the NO/M_5(sp) systems, corresponds to that of the E_{ads} values.

Regarding also the cases of the NO/M_5(tb) systems with M = Ir, Pt, and Au, the two types of the initial geometries in which a NO molecule was located at the above the bridge site of the precious metal M_5(tb) clusters were taken into account, in addition to our
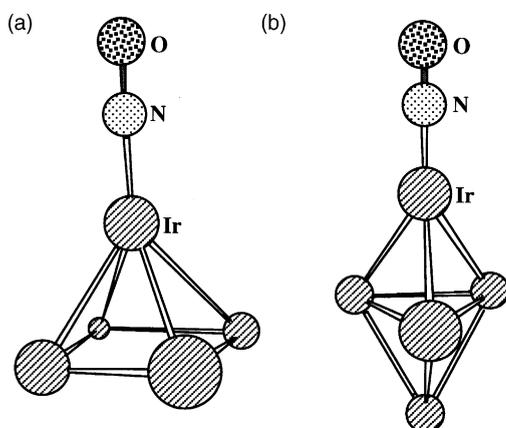
Fig. 2. Schematic views showing the most stable adsorption states of NO molecules on (a) $Ir_5(sp)$ and (b) $Ir_5(tb)$ clusters, respectively.

previous investigation [25]. In the series of the $NO/Ir_5(tb)$ systems, similar to the cases of the $NO/Rh_5(tb)$ and $NO/Pd_5(tb)$ systems, the linear adsorption state of the NO molecule on the $Ir_5(tb)$ cluster is the most thermodynamically favorable (-73.7 kcal/mol; see Fig. 2(b)). The bond distance of the Ir–N bond is 1.757 Å, which is very close to that of the $NO/Ir_5(sp)$ system. The apex atom of the $Ir_5(tb)$ cluster in the adsorbed system possesses $+0.30$ of the atomic charge. This atomic charge is greater than that of the $NO/Ir_5(sp)$ system ($+0.18$) and suggests the appearance of the larger π back-donation from the Ir atom to the adsorbed NO molecule in the $NO/Ir_5(tb)$ system. In the cases of the $NO/Pt_5(tb)$ systems, it is again seen that the linear adsorption mode of the NO molecule on the $Pt_5(tb)$ cluster is the most stable one from the energetic point of view (-61.5 kcal/mol). The distance of the Pt–N bond is 1.781 Å, which is close to that of the $NO/Pt_5(sp)$ system. The atomic charge on the apical Pt atom in the $NO/Pt_5(tb)$ system is $+0.27$. The E_{ads} values for the $NO/Au_5(tb)$ systems indicate that the significantly bent adsorption structure of the NO molecule on the $Au_5(tb)$ cluster obtained by starting from the BR_L initial geometry is the most favorable (30.2 kcal/mol). In spite of the initial geometry, one Au–N bond was formed in this adsorption state. The bond length is 1.977 Å and is close to that of the $NO/Au_5(sp)$ system (1.982 Å). The tendency of the coordination number of the NO molecule to the $Au_5(tb)$ cluster is different from that of the

$NO/Au_5(sp)$ systems. However, it is found that except for the adsorption states obtained by starting from the 3F_L and 3F_B initial geometries (see [25]), the numbers of the Au–N bonds in the present $NO/Au_5(tb)$ systems are 1.

From the comparison of the absolute values of E_{ads} for the $NO/M_5(tb)$ systems with M = Ir, Pt, and Au, it is revealed that the order of the energetic stability on the $NO/M_5(tb)$ systems can be demonstrated as Ir > Pt > Au. In the case of the $NO/M_5(tb)$ systems with M = Ir, Pt, and Au, the order of the M–N distances is in agreement with that of the E_{ads} values. The present study has considered the additional initial geometries for various NO/M_5 systems, comparing with the previous study [25], in order to scan more accurately potential energy surfaces for the NO adsorption. The entire order of the E_{ads} values for the $NO/M_5(tb)$ systems (M = Ir, Pt, and Au) is the same as the previous findings [25], although the most stable adsorption mode of the NO molecule on the $Au_5(tb)$ cluster changed.

According to the entire comparison of the E_{ads} values shown in Table 2, it is evident that the order of the thermodynamic stability of the adsorption states of the NO molecules on the $M_5(tb)$ clusters can be represented as Ir > Rh > Pt > Pd > Ag > Au. This partly agrees with that found for the $NO/M_5(sp)$ systems.

Let us consider the electronic structures from the viewpoint of the electronic population of the adsorbed NO molecules on the $M_5(tb)$ clusters. Similarly to the above considerations for the $NO/M_5(sp)$ systems, the most energetically stable adsorption states of the NO molecules on each $M_5(tb)$ cluster obtained from the six kinds of initial geometries were used to the Mulliken population analysis. As shown in Table 3, an considerably large π back-donation from the $Pd_5(tb)$ cluster to the $2\pi^*$ orbital in the adsorbed NO molecule appears. Nevertheless, all $NO/M_5(tb)$ systems demonstrate the donation and π back-donation. The reason why the substantially large π back-donation was occurred in the case of the $NO/Pd_5(tb)$ system is not still clear. At least, however, the relatively large values of the positive atomic charge on the apical Ir atom in the $NO/Ir_5(tb)$ system may be able to explain by the back-donation from the Ir atom to the $2\pi^*$ orbital of the adsorbed NO molecule with the large amount of electrons (0.92).

An important observation should be mentioned. Comparing all E_{ads} values estimated, it is concluded that the Ir_5 cluster possesses the highest affinity to a NO molecule. This observation was already pointed out by our preliminary study [25]. In addition, the similar nature of the Ir cluster was also revealed theoretically by our group, when tetrahedral M_4 clusters were considered [24]. Combining these previous findings with the present results, we may be able to conclude that the highest ability of the Ir cluster regarding the NO adsorption does not depend on either the shape of the Ir cluster or the number of atoms in the model cluster. We would like to stress again that such a property concerning the NO adsorption, which the Ir cluster possesses, is expected to be responsible for the high catalytic performance on the SCR of NO_x under lean-burn conditions.

5. Conclusions

In summary, in the present study an attempt has been made to screen suitable noble-metal catalysts for the SCR of NO_x by combinatorial computation chemistry approach. As a model catalyst system, a pentaatomic metal clusters (M_5) with square pyramidal (sp) and trigonal bipyramidal (tb) geometries were considered as the substrate while linear and bend geometries were considered for the adsorbent NO molecule. Among the various metal clusters employed in this investigation, it was found that regardless of the cluster size and geometry as well as the adsorption models, the Ir cluster is energetically more favorable than the others. The results are in good agreement with the experimental results as well as with the calculations performed using a tetraatomic cluster model. However, from the viewpoint of designing highly efficient or new catalyst systems for the $deNO_x$ reaction under lean-burn conditions, it is important to rationalize the stability the clusters for the activation of NO over a wide range of elements and different cluster geometries. Such a study is currently in progress.

References

[1] R.B. van Dover, L.F. Schneemeyer, R.M. Fleming, Nature 392 (1998) 162.

[2] E. Danielson, J.H. Golden, E.W. McFarland, C.M. Reaves, W.H. Weinberg, X.D. Wu, Nature 389 (1997) 944.

[3] G. Briceno, H. Chang, X. Sun, P.G. Schultz, X.D. Xiang, Science 270 (1995) 273.

[4] K. Yajima, Y. Ueda, H. Tsuruya, T. Kanougi, Y. Oumi, S. Salai Cheettu Ammal, S. Takami, M. Kubo, M. Miyamoto, Appl. Catal. A 194–195 (2000) 183.

[5] S. Sakahara, K. Yajima, R. Belosludov, S. Takami, M. Kubo, A. Miyamoto, Appl. Surf. Sci. 189 (2002) 253.

[6] J.T. Kummer, Prog. Energ. Combust. 6 (1980) 177.

[7] K.C. Taylor, Catal. Rev.-Sci. Eng. 35 (1993) 457.

[8] M. Shelef, G.W. Graham, Catal. Rev.-Sci. Eng. 36 (1994) 433.

[9] E.A. Hyde, R.J. Rudham, Chem. Soc., Faraday Soc. 1 (1984) 531.

[10] S.H. Oh, C.C. Eickel, J. Catal. 128 (1991) 526.

[11] S.S.C. Chuang, C.-D. Tan, Catal. Today 35 (1997) 369.

[12] E. Nová k, d. Sprinceana, F. Solymosi, Appl. Catal. A 149 (1997) 89.

[13] D.R. Rainer, M. Koranne, S.M. Vesecky, D.W. Goodman, J. Phys. Chem. B 101 (1997) 10769.

[14] K.C. Taylor, in: J.R. Anderson, M. Boudart (Eds.), Catalysis Science and Technology, Springer, Berlin, 1984, p. 120.

[15] M. Iwamoto, H. Hamada, Catal. Today 10 (1991) 57.

[16] W. Held, A. Konig, T. Richter, L. Puppe, Soc. Automotive Eng. (1990) 900496.

[17] L.J. Lobree, I.-C. Hwang, J.A. Reimer, A.T. Bell, Catal. Lett. 63 (1999) 233.

[18] R.Q. Long, R.T. Yang, Chem. Commun. (2000) 1651;
R.Q. Long, R.T. Yang, J. Catal. 207 (2002) 274.

[19] C. Wögerbauer, M. Maciejewski, A. Baiker, U. Göbel, J. Catal. 201 (2001) 113.

[20] C. Wögerbauer, M. Maciejewski, A. Baiker, Appl. Catal. B 3 (2001) 11;
C. Wögerbauer, M. Maciejewski, A. Baiker, J. Catal. 205 (2001) 157.

[21] N. Miyoshi, S. Matsumoto, K. Katoh, T. Tanaka, J. Harada, N. Takahashi, K. Yokota, M. Sugiura, K. Kasahara, Soc. Automotive Eng. (1996) 900496.

[22] M. Nawdali, H. Praliand, M. Primet, Top. Catal. 16–17 (2001) 199.

[23] M. Hon, A. Okumura, H. Goto, M. Horiuchi, SAE 972850 (1997) 1.

[24] A. Endou, N. Ohashi, K. Yoshizawa, S. Takami, M. Kubo, A. Miyamoto, E. Broclawik, J. Phys. Chem. B 104 (2000) 5110.

[25] A. Endou, N. Ohashi, S. Takami, K. Momoji, A. Miyamoto, E. Broclawik, Top. Catal. 11–12 (2000) 271.

[26] E.J. Baerends, D.E. Elis, P. Ros, Chem. Phys. 2 (1973) 41.

[27] S.H. Vosko, L. Wilk, M. Nusair, Can. J. Phys. 58 (1980) 1200.

[28] A.D. Becke, Phys. Rev. A 38 (1988) 3098;
J.P. Perdew, Phys. Rev. B 33 (1986) 8822.

[29] K.P. Huber, G. Herzberg, Molecular spectra and molecular structure, in: Constants of Diatomic Molecules, vol. 4, Van Nostrand, Princeton, 1979.

[30] A. Stirling, I. Pápai, J. Mink, J. Chem. Phys. 100 (1994) 2910.

[31] H. Munakata, T. Kakumoto, J. Baker, J. Mol. Struct. (THEOCHEM) 391 (1994) 231.

[32] S.E. Deutsch, F.-S. Xiao, B.C. Gates, J. Catal. 170 (1997) 161.

[33] S.E. Deutsch, G. Mestl, H. Knözinger, B.C. Gates, J. Phys. Chem. B 101 (1997) 1374.

[34] A. Zhao, B.C. Gates, J. Catal. 168 (1997) 60.

[35] O. Alexeev, G. Panjabi, B.C. Gates, J. Catal. 173 (1998) 196.

[36] S.H. Yang, D.A. Drabold, J.B. Adams, P. Oredejón, K. Glassford, J. Phys. Condens. Matter 9 (1997) L39.

[37] N. Materer, A. Barbieri, D. Gardin, U. Starke, J.D. Batteas, M.A. van Hove, G.A. Somorjai, Surf. Sci. 303 (1994) 319.

[38] D. Loffreda, D. Simon, P. Sautet, J. Chem. Phys. 103 (1998) 6447.

[39] M.H. Tsai, K.C. Hass, Phys. Rev. B 51 (1995) 14616.

[40] W. Mannstadt, A. Freeman, J. Phys. Chem. B 55 (1997) 13298.

[41] G. Blyholder, J. Phys. Chem. 68 (1964) 2772.